Bulletin of Pure and Applied Sciences
Geology, Vol.45F, No.2,
July-December 2026: P.1-28
Original Article

Print version ISSN 0970 4639
Online version ISSN 2320 3234
Available online at www.bpasjournals.com

HETEROGENEITIES AND ROCK TYPES CHARACTERISTICS IN A TIDE-DOMINATED ESTUARINE SANDSTONE RESERVOIR DEPOSIT, COASTAL SWAMP DEPOBELT, NIGER DELTA BASIN, NIGERIA

Raphael Oaikhena Oyanyan*

Author's Affiliations:
Department of Physics and Geology, Federal University Otuoke, P.M.B. 126, Yenagoa, Bayelsa State, Nigeria.

***Corresponding Author: Raphael Oaikhena Oyanyan,** Department of Physics and Geology, Federal University Otuoke, P.M.B. 126, Yenagoa, Bayelsa State, Nigeria.
E- mail: oyanyanro@fuotuoke.edu.ng

Received on 24.07.2026, Revised on 14.09.2026, Accepted on 17.10.2026

How to cite this article: Oyanyan R.O. (2026). Heterogeneities and Rock types Characteristics in a tide-dominated Estuarine Sandstone Reservoir Deposit, Coastal Swamp Depobelt, Niger Delta basin, Nigeria. *Bulletin of Pure and Applied Sciences- Geology,* 45F (2), 1-28

Abstract:
An oil-down-to and oil-up-to sandstone reservoir at the crest of a rollover anticline was characterised to document the petrophysical properties of the different sedimentary facies and to achieve optimum petroleum production. Characterisation methods include logs stacking pattern analysis, lithofacies analysis of cores, special core analysis data interpretations, evaluation/quantification of heterogeneity, and Winland r35 and hydraulic unit rock-typing. The depth zone of interest was interpreted as transgressive systems tract (TST) due to the backstepping logs' pattern. Twelve lithofacies described the cores, while the lithofacies characteristics/associations resulted in the identification of depositional environments that include fluvial channels and inner, outer and middle estuaries and transgressive and regressive offshore, transgressive offshore-transition and shoreface environments. Porosity and permeability values of all the sandstone facies indicate high reservoir quality due to moderated to well-sorted grains. Winland's R35 rock-typing categorised 75% of the rock to be mega-porous, but the twelve lithofacies, the Dykstra-Parson's coefficient of 0.84 of core permeability distribution and the normal probability plot of irreducible water saturation indicate a high level of heterogeneities, with potential for compartmentalization and consequent poor sweep efficiency. Hydraulic unit rock-typing categorised the reservoir into eight hydraulic units (HUs) based on flow zone indicators (FZIs). HU rock-types 1 to 6 are reservoir hydraulic flow units (HFU) with FZI that range from good (0.6 µm) to best (1.52 µm). The plot of hydraulic units against depth indicates fluctuating tidal current speed and energy as the dominant controls on reservoir quality. The HU 7 and 8 with FZI 0.24 and 0.03 µm, respectively, serve as baffles and compartmentalized the reservoir into three compartments as non-reservoirs. Perforating the depth interval with the best HFUs in each compartment is a beneficial option for optimum petroleum production. The multiple linear regression machine learning algorithm predicted the flow zone indicators of the same reservoir in a distant non-cored oil well.

Keywords: *Lithofacies variability; estuary; depositional environments; pore-throats; hydraulic flow units; compartmentalization*

1. INTRODUCTION

Sandstone reservoirs deposited in a tide-dominated coastal estuary are documented to form petroleum reservoirs with good to excellent quality due to the generally moderate to well-sorted fine- to coarse-grained texture (Buatois, 1999; Zhang et al., 2022; Jiwei et al., 2025). It is also documented, just like the wave-dominated estuarine sandstone reservoirs, to exhibit mesoscale to

microscale heterogeneities due to the mixture of fluvial influence and hydrodynamics of tides and wave processes in the deposition (Galloway and Hobday, 1996; Buotois, 1999; Mack et al., 2003; Bello et al., 2024). It is documented that heterogeneity is at its greatest in reservoirs that were deposited under the influence of tidal currents, where there is common intercalation of sandstones and mudstones across a wide range of scales (Nio and Yang, 1991). Therefore, studying the complexities in the scale of heterogeneities inherent in petroleum-rich tide-dominated estuarine reservoirs via adequate fine-scale characterisation of their storage and flow properties has become a very crucial and necessary prerequisite if optimum recovery or production of the petroleum can be achieved (Jiwei et al., 2025).

The Niger Delta basin sediments, in general, represent a coalescence of five delta lobes fed by four rivers (Ejedawe, 1981). The deltaic progradation was maintained through a steady increase in sediment supply and the combined influence of eustatic cyclicity, local deltaic autocyclic processes and local tectonics that provided the accommodation for the preservation of the sediment supplied (Knox & Omatsola, 1987; Reijers, 2011). The allocyclic processes resulted in the deposition of the regional correlative shale markers, while the autocyclic processes such as delta lobe switching, local growth fault subsidence, waves and tidal processes resulted in the deposition of fieldwide to inter-well correlative sandstones and shales as well as intra-reservoir shales responsible for mesoscale-microscale reservoir heterogeneities and intra-sandbody compartmentalization (Oyanyan and Oti, 2016). Marine transgression, or the landward movement of the shoreline associated with the rate of increase in accommodation over the rate of sediment supply during the periodic eustatic sea level rise or increased local tectonic subsidence, resulted in the deposition and preservation of transgressive systems tracts (TST) sediment in the drowned river mouths/channels, called estuaries (Owejemi and Willis, 2006; Catuneanu, 2006; Tessier, 2012). Generally, vertical reservoir compartmentalization potential is relatively high in TST sediments because of the enhanced preservation potential of flooding surface shales (Ainsworth, 2010).

It is important to note that, unlike the deposits of components of a delta such as river mouth bar/delta front, regressive distributary channel and shoreface, the sedimentological and petrophysical characteristics of estuarine deposits are scarce in the Niger Delta Basin literature. The few documented cases are either wave-dominated or tide-dominated estuaries. The wave-dominated estuarine deposits were deposited in a wave-dominated river-mouth regressive setting but in a general shoreline transgressive setting and characterised by backstepping successions of coarsening-upward beaches or bayhead deltas (Oyanyan et al., 2023). The tide-dominated estuarine sediments were deposited in a tide-dominated river mouth in a shoreline transgressive setting and are characterised by successions of backstepping finning-upward sandstone deposits (Oyanyan and Oshinowo, 2026).

Oyanyan and Oshinowo (2026) interpreted petroleum-rich Miocene D1 sandstone at the Coastal Swamp Depobelt of the Niger Delta basin as tide-dominated estuary deposits (transgressively backfilled fluvio-estuarine distributary channels) based on lithofacies characteristics. They identified variability in lithofacies and mud drapes in some depositional facies that suggest heterogeneities in the reservoir's petrophysical quality that can impact petroleum production and therefore asserted that adequate characterisation of flow units would be a necessary requirement to achieve high sweep efficiency for optimum petroleum recovery or production. Optimum petroleum production from a reservoir is having high sweep efficiency, resulting in little or no bypassed oil in the reservoir or a negligible amount of trapped oil left behind in the reservoir. Therefore, this paper presents the results of a study of the Miocene D1 sandstone aimed at documenting the sedimentological control on reservoir quality as well as the detailed characterisation of the flow units. The objectives of the study include the following: 1. Correlation of the reservoir depth interval across the field. 2. Identification of the variation of petrophysical parameters with different lithofacies and lithofacies

associations/depositional environments, 3. Quantification and evaluation of the heterogeneities in the petrophysical properties of the rock, 4. Identification of rock types and flow units with distinct flow capacities in the reservoir, 5. Determination of the sedimentological control on the distribution of flow units. 6. Identification of intra-reservoir compartments and the determination of a well perforation depth interval that can result in optimum petroleum recovery, based on the vertical distribution of the flow units.

1.2 Location of Study Area and Geologic Setting

The study oilfield is in the Coastal Swamp depobelt of the Niger Delta basin of Nigeria at the Gulf of Guinea in West Africa (Fig. 1a). It currently has four wells producing petroleum from Miocene sandstone reservoirs of one depositional sequence. The oil field is divided into three fault blocks by one east-to-west trending major growth fault and two synthetic growth faults, and all the study oil wells are within the central fault block (Fig. 1b). The actual name of the oilfield and that of the operator are concealed for propriety's sake.

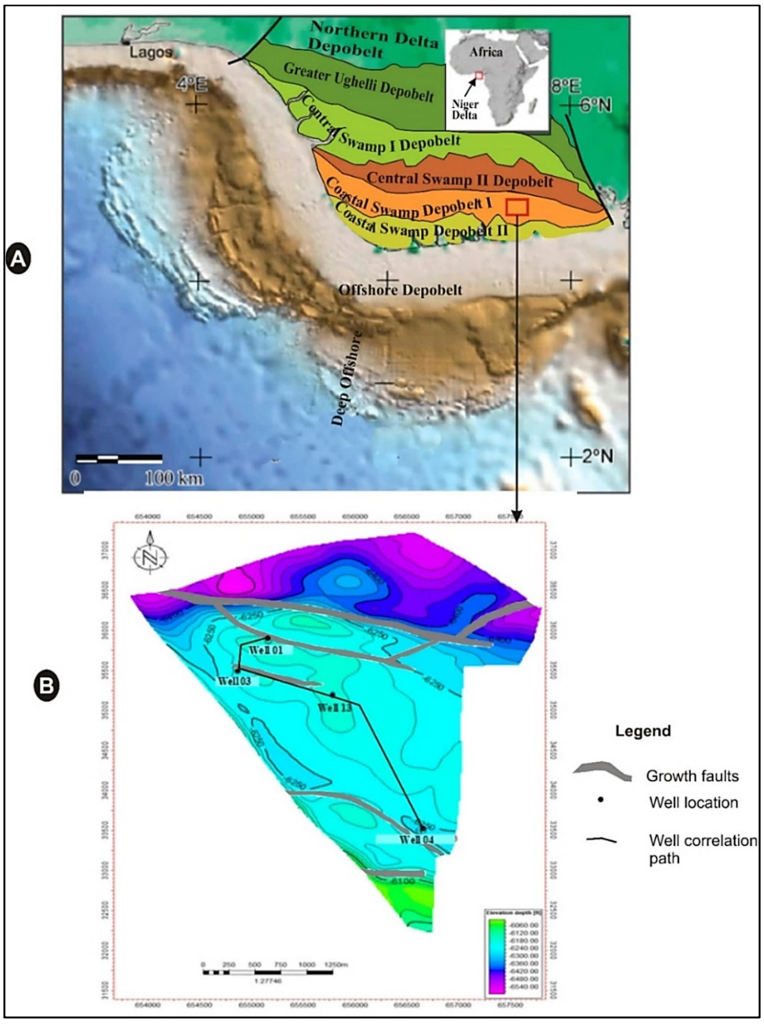


Figure 1: Study area location maps. **A.** Shows the depobelts in the Niger Delta basin, the study field depobelt and the location of the basin at the Gulf of Guinea in West Africa (Modified after Smith and Sandwell 1997; Doust and Omatsola 1989). **B.** The structural map of the study field showing oil wells, growth faults distributions and the path of well logs correlation.

The study tide-dominated D1 sandstone reservoir is part of the Agbada Formation, one of the three lithostratigraphic units of the Niger Delta Basin (Short and Stauble, 1967; Weber and Daukoru, 1975). The Agbada Formation is a paralic marine deposit consisting of alternations of units of sandstone and shale that formed petroleum reservoirs and seals, respectively. It has a maximum thickness of 4000 m with a diachronous age that ranges from Eocene to Recent. Underlying the Agbada Formation is an overpressured marine deposit called the Akata Formation, consisting dominantly of shale, believed to be the major source rock for petroleum in the basin. It has a maximum thickness of 6500 m and an age that ranges from Palaeocene to Recent. Overlying the Agbada Formation is the coastal plain sand deposit called the Benin Formation, consisting of continental fluvial sands/gravels and back swamp deposits, with a maximum thickness of 2000 m and an age that ranged from Eocene to Recent.

The tectonic evolution of the Niger Delta Basin is linked to the formation of the Cretaceous Benue Trough that runs diagonally across Nigeria from the northeast to the southwest. The Benue Trough represents the failed arm of the triple junction during the Late Mesozoic separation of the South American plate from the African plate (Whiteman, 1982). The Niger Delta basin that is located at the southward end of the Benue Trough was built over the collapsed continental margin of the South Atlantic that resulted from the successful separation of the two plates (Doust and Omatsola, 1989). The Palaeocene major marine transgression into the Benue Trough that was followed by episodic regression that began in the late Palaeocene or early Eocene and continued till recent times initiated the evolution of the Niger Delta basin's sedimentary sequences. The basin is divided into mini basins called 'depobelts' by east–west trending regional and counter-regional growth faults, with the three diachronous lithostratigraphic units represented in each depobelt (Knox and Omatsola, 1987) (Fig. 1a).

2. DATA SET AND METHOD OF STUDY

The data set provided for this study includes a structural map of the field showing structural elevations, growth faults and oil wells' distribution (Fig. 1b); 60 ft (18.3 m) core pictures of slabbed full-diameter cores of depth of interest in well 13; and gamma ray, resistivity, neutron, density and water saturation logs of four wells as well as the special core analysis data of 61 core samples that include permeability, porosity and irreducible or connate water saturations.

To achieve the aim and objectives of the study, the study was divided into sections that include the evaluation of megascopic, macroscopic and microscopic reservoir heterogeneities (Weber, 1986; Lasseter *et al*., 1986; Ravalec et al., 2014); the determination of depositional control on hydraulic flow unit distribution; and the identification of intra-sandbody compartmentalisation and the proposition of a well perforation guide for optimum petroleum production.

Macroscopic heterogeneities correspond to the inter-well spacing scale and can be detected via well log correlations (Ravalec et al., 2014). Therefore, the entire D sandstone reservoirs and cored D1 sandstone depth zone in well 13 were identified with the gamma ray value that ranges from 30 to 65 API. The gamma ray log stacking pattern was analysed to determine the palaeo-depositional trend of the D sandstone reservoirs using the scheme of Cant (1992) and then identified the systems tract and bounding surface based on the principle of sequence stratigraphy (Catuneanu, 2006). Correlation of strata is the first step in defining potential connectivity or predicting compartmentalization (Ainsworth, 2010). Therefore, D sandstone reservoir intervals were then correlated across the other three oil wells in line with the detailed sequence stratigraphic fieldwide well log correlations of Oyanyan and Oshinowo (2026). The resistivity logs were used to identify the presence of petroleum in D reservoir sandstone, while the neutron and density logs differentiated between crude oil and gas in each of the wells, if any, based on methods duly explained by Dewan (1983).

Macroscopic and mesoscopic reservoir heterogeneities are detected at the level of cores through the identification of lithofacies/depositional environments and evaluation of cores' petrophysical properties, respectively (Ravalec et al., 2014). To analyse lithofacies variability in the cored interval, the lithofacies identified by Oyanyan and Oshinowo (2026) were also identified but differentiated with the addition of core petrophysical properties that include core porosity, core permeability and water saturations. The different types of lithofacies were identified based on lithology, colour, primary sedimentary structure, bioturbation and ichnofossils. The characteristics of lithofacies and association of lithofacies were used to infer the environment of deposition. The vertical occurrence of lithofacies, their physical and biological properties and environment of deposition were documented in a sedimentary log.

Core porosity and permeability values were qualitatively evaluated with histograms/cumulative frequency distributions and cross-plot analysis. The coefficient of permeability variation of Dykstra and Parsons (1950) as explained by Jensen *et al*. (2000) was used to quantify permeability heterogeneity. The Dykstra-Parsons coefficient (Vdp) is defined as follows:

$$V = \frac{k_{50} - k_{84.1}}{k_{50}} \quad \ldots\ldots (1)$$

Where:

k_{50} = Median reservoir permeability.

$k_{84.1}$ = Permeability at the 84.1 percentile

The Dykstra-Parsons coefficient values range from a minimum of 0 (pure homogeneous) to a maximum of 1.0 (heterogeneous). Most reservoirs have Vdp = 0.5 to 0.9.

Microscopic reservoir heterogeneities occur at the level of pores and grains (Ravalec et al., 2014). It was evaluated by the determination of petrophysical rock-type distributions in the cores. 'Petrophysical rock types here means the rock units that have similar storage and flow properties. It was first qualitatively evaluated with a normal probability plot of the irreducible water saturation values of the core samples. The rock types were further quantitatively determined using Winland's and hydraulic units' methods, described as follows:

(a) Winland method: It is the empirical method that links pore-throats in a unit of rock to porosity, permeability and capillary pressure (Gunter et al. 1997). The empirical relationship of Dale Winland of Amoco linked pore-throat radius at 35% mercury saturation with core porosity and permeability with the following popular equation, called the Winland equation, published by Kolodzie (1980).

$$\text{Log}_{R35} = 0.732 + 0.588 \log K_{air} - 0.864 \text{Log}\, \phi_{core} \quad \ldots\ldots\ldots (2)$$

Where R35 = the pore aperture radius corresponding to the 35th percentile of mercury saturation in a mercury porosimetry test, K_{air} = the uncorrected air permeability (in md), and ϕ_{core}= core porosity (in per cent).

Petrophysical Winland rock types were classified based on pore throat sizes into mega-porous (>10 µm), macro-porous (between 2.0 and 10 µm), meso-porous (between 0.5 and 2.0 µm), micro-porous (between 0.2 and 0.5 µm), and nanoporous (<0.2 µm) rock types (Boada et al., 2001). Mega-porous rock was taken as a very high-quality reservoir, while macroporous- a high quality reservoir, mesoporous- moderate reservoir, macroporous-limited reservoir potential and nanoporous as non-reservoir.

(b) Hydraulic Unit method: This is Amaefule *et al.'s* (1993) petrophysical rock-typing method based on Reservoir Quality Index (RQI) and Flow Zone Indicator (FZI). It is a method that divides the reservoir interval into hydraulic (flow) units. A hydraulic unit (HU) has been defined as a representative elementary volume of the total reservoir rock within which geological and petrophysical properties that affect fluid flow are internally consistent and predictably different from the properties of the other rock volume (Amaefule et al., 1993). It provides a physical measure of the rock flow and storage properties at current

conditions and reflects the current pore structure as modified by diagenesis (Rushing *et al*., 2008). FZI is a function of mineralogy and texture and reflects the relationship between pore throats, while RQI is a close approximation of the average pore throat (Abbaszadeh et al., 1995; Rushing *et al*., 2008; Oyanyan and Oti, 2016). FZI and RQI were obtained with the equations 3-5 below:

$$FZI = RQI / PHIZ \quad \ldots\ldots\ldots (3)$$

$$RQI\ (microns) = 0.0314\ \sqrt{v}\ (K/\phi_e) \quad \ldots\ldots\ldots (4)$$

$$PHIZ = \Phi z = (\phi_e / 1 - \phi_e) \quad \ldots\ldots\ldots (5)$$

For the prediction of K, the combination of equation of 3 and 4 gives equation 6.

$$K = = \phi_e * ((FZI * \Phi z)^2) / 0.00098596 \quad \ldots\ldots\ldots (6)$$

Where:

FZI = Flow zone indicator

RQI = Rock quality index

PHIZ = Zone porosity (*ΦZ*). Also called normalized or index porosity.

ϕ_e = Core porosity in fraction.

Normal probability plotting and graphical clustering were both used to classify the FZI values into hydraulic units (HU) and rock types, with the best method finally adopted in the identification of flow units.

A cross-plot of core porosity, core permeability, r35 and flow zone indicator values was done against each other and depth to evaluate for correlation. Hydraulic units were plotted against depth to determine the depositional control on flow unit distributions and intra-sandbody compartmentalization.

To predict pore-throat size distribution and hydraulic flow units of the same reservoir in a non-cored well that is not in pressure communication with the cored well due to heterogenities, multiple linear regression (MLR) algorithims were developed (Orlov, 1996; (Draper and Smith, 1998). The so-called supervised machine learning MLR models or algorithms were trained using gamma ray and bulk density log data as the independent or predictor variable, while R35, FZI and core permeability values were used as the dependent variable (Wendt *et al*., 1986).

3. RESULTS AND INTERPRETATIONS

3.1 Megascopic heterogeneities

3.1.1 Well logs correlation and Systems tract

The correlations of sandstone reservoirs within the stratigraphic framework across the four oil wells indicate megascopic heterogeneities (Fig. 2). It shows heterogeneities at both interwell and fieldwide scales (Weber, 1986). Fieldwide correlating flooding surface shales divided the D sandstone reservoir into three compartments (D1, D2 and D3) corresponding to inter-parasequence reservoir compartmentalization (Ainsworth, 2010). The D1 reservoir is divided into D1a and D1b by a layer of shale that is correlative to all the wells except Well 04, which could be due to a missing section associated with a fault to suggest structural compartmentalization or a depositional pinch-out to suggest inter-sand-body compartmentalization (Ainsworth, 2010). The correlation of the subunits of the D sandstone reservoir across all the oil wells indicates a layer-cake stratigraphic architecture (Weber and van Geuns, 1990).

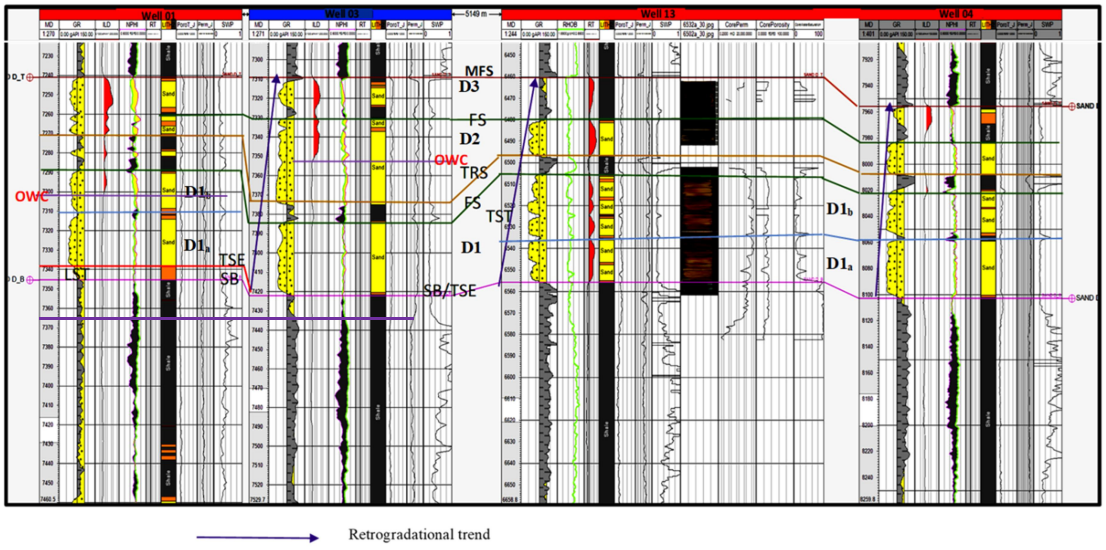
The gamma ray log motifs of the reservoir sands show an overall upward-fining sequence that consists of a succession of two upward-fining and sandstone-thickness-decreasing sequences and therefore represents backstepping stacking patterns or a retrogradational trend typical of a transgressive systems tract (TST) (Cant, 1992; Catuneanu, 2006). The basal upward finning sequence is the cored depth interval. The TST is bounded on top and bottom by a maximum flooding surface (MFS) and a transgressive surface of erosion (TSE), respectively. A thin unit of lowstand systems tract (LST) underlay the TST only in well 01. For the detailed sequence stratigraphic analysis of the field, please see Oyanyan and Oshinowo (2026).

3.1.2 Petroleum Occurrence and Distribution

Resistivity and water saturation logs indicate that petroleum is not uniformly distributed across the D sandstone reservoirs in all the wells (Fig. 2). The oil down-to and oil up-to D3 sandstone reservoirs are correlative across all the wells. The D2 sandstone reservoir is a water-bottom petroleum-bearing reservoir in wells 01 and 03 but an oil-down-to and oil-up-to in well 13. The cored D1 reservoir is oil down-to and oil up-to in wells 13, water-bottom in well 01 and dried in other wells. All the sandstone reservoir units (D1, D2 and D3) in well 13 are oil-down to and oil-up to. These characteristics can be attributed to the location of well 13 at the crest of the structure, where the effects of gravity segregation and force of buoyancy migrate the lighter petroleum to a position of high elevation and above water. Apart from the effect of gravity segregation, the vertical distribution of petroleum in well 13 and the uneven aerial distribution of petroleum in the D2 and D1 reservoirs can be attributed to megascopic heterogeneities.

3.2 Macroscopic and mesoscopic heterogeneities

Macroscopic and mesoscopic heterogeneities are interwell and wellbore-scale heterogeneities, respectively (Weber, 1986; Ravalec et al., 2014). They determine the amount of displacing fluid and the amount of bypassed oil (Ravalec et al., 2014). They were evaluated using core properties that include wellbore lithofacies distribution and environments of deposition, porosity, permeability and water saturation correlative to other wells.



Colour code of lithology and fluid: Yellow = Sandstone, Dark grey =Mudstone/shale, Orange = Shaley sandstone, Red = Hydrocarbon. Acronyms: MFS = Maximum flooding surface, FS = Flooding surface, TRS = Tidal ravinement surface, TSE = Transgressive surface of erosion, SB = Sequence boundary, TST = Transgressive systems tract, LST = Lowstand systems tract.

Figure 2: Well logs correlation of D reservoir sandstone within a sequence stratigraphic framework, showing cored intervals, bounding surfaces, depositional trend and transgressive systems tract as well as resistivity logs indicating depth interval of petroleum occurrence. Megascopic heterogeneities include lateral discontinuities of individual strata and pinchouts, oil water contacts (OWC) and depositional trends variations, reservoir compartmentalization. Depth of wells are measured in feet.

3.2.1 Lithofacies types and variability with petrophysical properties

Twelve lithofacies were identified in the 60 ft (18.3 m) cores of the D1 sandstone reservoir (Fig. 2). The detailed characteristics of the lithofacies and the depositional environments are well documented by Oyanyan and Oshinowo (2026). The summary of the lithofacies and variability with petrophysical properties is presented in Table 1.

Table 1: Summary of lithofacies sedimentological description, mean Petrophysical properties and depositional environments (after Oyanyan and Oshinowo, 2026)

Lithofacies No.	Lithofacies	Sedimentological description and core petrophysical properties	Deposition process	Bed sets/sub environ.	Depo. environ.
1.	Dark grey mudstone	Mudstone, dark grey and massive (Fig. 3A). B = 0. Porosity (Φ) = 7.5 %, Permeability (K) = 0.2 md, Water saturation (Sw) = 81.8%.	Rapid deposition of suspended load in a low-energy environment	Open marine	Transgressive offshore
2.	Bioturbated Sideritic mudstone	Pervasive greyish-brown siderite in dark grey mudstone. B = 0, (Fig. 3A). Φ = 27%, K = 949 md, Sw = 40.1%.	Suspension fall-out and diagenetic mineral chemical precipitation	Transgressive tidal flat	Transgressive offshore transition zone.
3.	Mud-draped cross laminated sandstone	Sandstone, fine- to very fine-grains, pervasive mud drapes and cross laminations. *Ophiomorpha nodosa* and *Ophiomorpha irregulaire*. BI = 1, (Fig. 3A). Φ = 30 %, K = 3786.1md, Sw = 12.3 %.	High energy deposition with intermittent low-energy deposition periods associated with slack water conditions in subtidal zone		Tide dominated transgressive shoreface.
4.	Cross bedded sandstone	Sandstone, light brown to light grey, fine to very coarse grains, very thin to medium beddings, rare sigmoidal thin cross beddings, rare double mud drapes and abundant reactivation surfaces. A rare diminutive *Bergaueria* burrow. B1 = 0 – 1, (Fig. 3A). Φ = 31.02%, K = 4834.99 md, Sw = 31.4 %,	Dune/bar forms migration and erosion of top of dune by high energy tidal current under subtidal condition	Tidal sandbars	Outer estuary.
5.	Heterolithic mudstone.	Alternating very fine-grained sandstone and shale, lenticular and flaser beddings. *Rhizocollarium, Planolite*	Migration of sandy ripples alternating with deposition of	Tidal flat	Estuary margin

		and *Teichichnus.* BI = 2 – 3, (Fig. 3A). Φ = 17.0%, K = 1630 md.	mud and silt from suspension under variable energy condition		
6.	Massive bedded sandstone	Sandstone, Light brown to greyish brown, massive and planar/undular erosion base. Rare Tubular tidalite. BI = 1 – 0, (Fig. 3A). Φ = 26.4 %, K = 6720 md, Sw = 25.2 % .	Rapid depositions of breaking tidal bores (very high energy tidal currents).	Tidal- bore deposits	Middle estuary
7.	Thickly interbedded sandstone and shale	Light brown sandstone, dark grey shale, carbonaceous shale, lenticular beddings and undulating sharp basal contact. Rare *Planolites* and siderite-filled burrows. BI = 2, (Fig. 3A). Φ = 13.2%, K = 1.1md, Sw = 68.2 %.	Sand deposition from tidal currents, mud fall out during slack-water intervals, and tractive sand deposition	Tidal flat	Middle estuary
8.	Channelized medium bedded cross-stratified sandstone.	Sandstone, Light grey to light brown, fine to coarse grains, high- to low-angle planar cross-beddings, cross-lamination, rare reactivation surfaces, rare double mud drapes, fluvial erosion surfaces and rare fluid mud-draped erosion surfaces. Are *Siphonichnus, Skolithos, Palaeophycus* and T*halassinoides* BI = 0-1, (Fig. 3A). Φ = 30.18%, K = 3538.7md, Sw = 6.6 %	Migrating two-dimensional dunes from high-energy unidirectional traction currents.	Tidal channel sandbars	Inner estuary
9.	Horizontal bedded sandstone	Sandstone, Light grey to light brown, fine to coarse grains, horizontal beddings, horizontal laminations and sharp basal contacts. Rare *Palaeophycus,* conjugate or y-shaped vertical burrows. BI = 0-1, (Fig. 3A). Φ = 26.85%, K =	Upper flow regime deposition	sandflats	Inner estuary

		2222.25md, Sw = 12.2 %			
10.	Heterolithic sandstone.	Light brown sandstone and light grey shale, inclined heterolithic stratification (IHS) and undulating basal contact. BI = 0-1, (Fig. 3A). Φ = 33.4 %, K = 1990md, Sw = 25.2 %	Deposition from helicoidal flow through a bend and lateral migration of the bend or meander channel	Subtidal point bars	Inner estuary
11.	Channelized thinly cross laminated sandstone.	Sandstone, fine to medium grains, light brown, parallel cross laminations and sharp/eroded basal surface. BI = 0, (Fig. 3A). Φ = 26.2%, K = 1807.5md, Sw = 14.0 %	Tractive deposition from unidirectional currents	Fluvial channel sand bars	Fluvial channel
12.	Heterolithic shale	Shale interlaminated with lenticular sandstone, parallel lamination and very gradual upward increase in sand thickness. Rare *Chondrites*. BI = 0 – 1 (Fig. 3A). Φ = 28.3%, K = 3.9md, Sw = 95.0 %	Gradual suspension load fall-out under low energy conditions	Open marine	Delta influenced offshore

3.2.2 Lithofacies associations (LFA) and variability with petrophysical properties

The characteristics and the association of twelve lithofacies resulted in the identification of eight depositional environments, in line with Oyanyan and Oshinowo (2026) (Fig. 3):

LFA 1: *Regressive offshore or Delta-influenced offshore.* Heterolithic shale (lithofacies 12) is characterised by a gradual upward increase in sandstone thickness and a downward increase in shale thickness typical of deltaic deposition (Nichols, 2009; Reijers, 2011). The facies is therefore interpreted to be deposited in regressive offshore or delta-influenced offshore (Table 1, Fig. 3). It is characterised by gamma ray values that decreased upward from 150 to 60 API (Fig. 2). Average cores' permeability, porosity and water saturation values are 3.9 md, 28.3% and 95.0%, respectively. Though the depositional facies have a high porosity value because of the upward increase in well-sorted sandstone thickness, the very poor permeability value and the almost 100% water saturation categorise the lithofacies as a non-reservoir for petroleum. The regressive offshore facies, however, formed the basal sealing depositional facies for the petroleum-bearing facies discussed below.

LFA 2: *Fluvial Channel.* The association of sandy heterolith (lithofacies 10) and channelized thinly cross-laminated sandstone (lithofacies 11) indicates sediment deposition in a fluvial channel (Table 1, Fig. 3). The depositional facies are characterised by channel surfaces, an upward-fining trend, upward-decreasing gamma ray log values from 35 to 58 API, and abruptly overlain the underlying facies with an erosive surface (Fig. 2). Average cores' permeability, porosity and water saturation values ranged from 1807.5 to 1990 md, 26.2 to 33.4 per cent, and 14.0 to 25.2 per cent, respectively. The permeability and

porosity values of the fluvial channel facies indicate very good reservoir quality. The water saturation value indicates that petroleum saturation in the lithofacies is up to 75% from top to bottom. As the bottommost reservoir, it thus means that the D1 reservoir is actually an oil down-to reservoir.

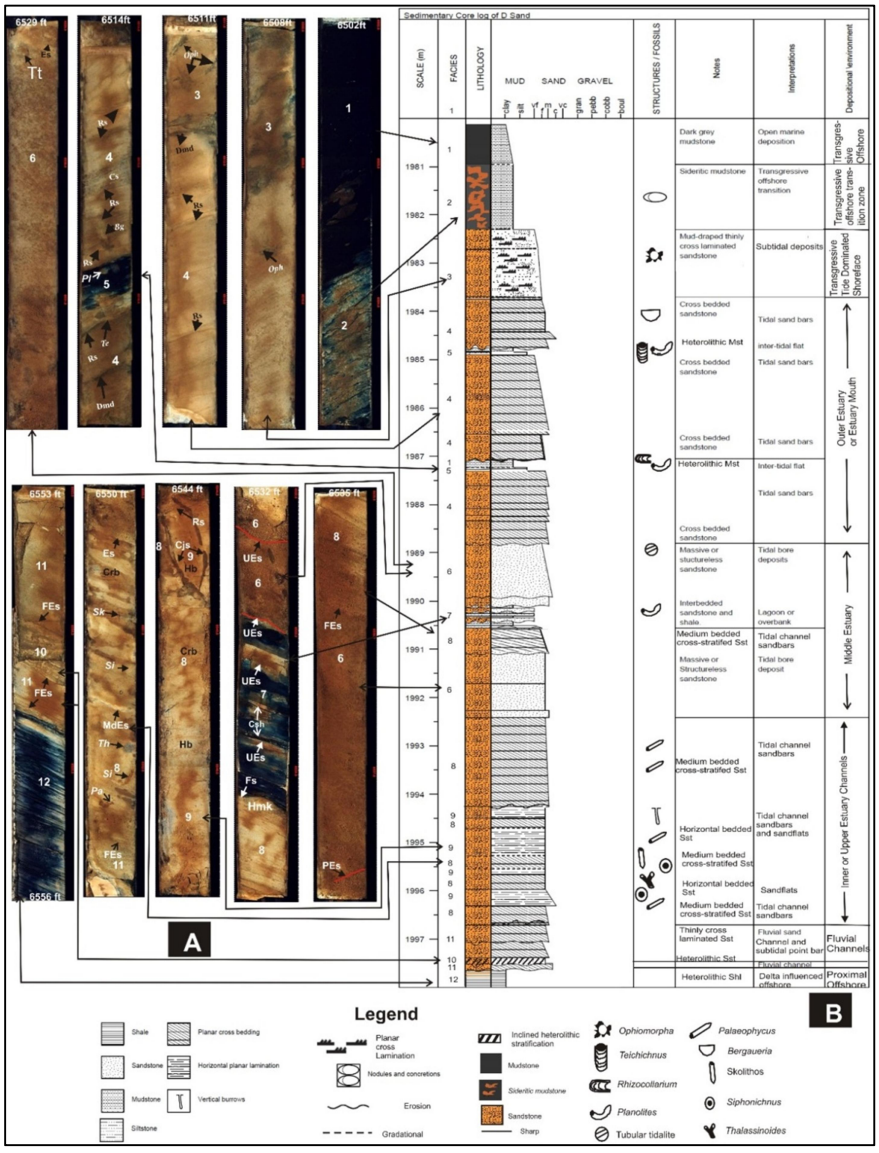


Figure 3: Core pictures in feet and Sedimentary log in meters of D1 sandstone reservoir depth interval 6,496 – 6556 ft (1,980 - 1998 m) of Well 13. (A) Diagnostic core pictures of lithofacies 1 to 12, with the black arrows point to their locations in the sedimentary log. (B) Sedimentary log showing lithofacies successions, lithofacies associations/depositional environments (modified after Oyanyan and Oshinowo, 2026). Acronym: Sst = Sandstone, Mst = Mudstone, Shl = Shale, CSh = Carbonaceous shale FS = Flooding surface, Rs = Reactivation surface, Es = Erosion surface, PEs = Planar erosion surface, UEs = Undular erosion surface, MdEs = Mud draped erosion surface Hmk = Hummock, Dmd = Double mud drapes,Crb = Cross bedding, Hb = Horizontal bedding, Crl = Cross laminated sandstone, Th = *Thalassinoides*, Si = *Siphonichnus*,Oph = O*phiomorpha*, Tt = *Tubular tidalite*, Pl = Planolites, Pa = *Palaophycus*, Sk = *Skolithos,Cjb* =Conjugate burrow.

LFA 3*: Inner or upper estuary.* The association of channelized medium-bedded cross-stratified sandstone (lithofacies 8) of tidal channel sandbars and horizontal-bedded sandstone

(lithofacies 9) of tidal sand flats indicates sediment deposited in the inner or upper estuary (Table 1, Fig. 3) (Dalrymple et al., 1992; Flemming, 2011). The depositional facies is generally a clean and well-sorted sandstone with an average gamma ray value of 30 API and overlies the fluvial channel facies. The inner estuary facies average core's permeability, porosity and water saturation values ranged from 2222.25 to 3538.7 md, 26.85 to 30.18%, and 6.6 to 12.2%, respectively. The high cores' permeability and porosity values indicate a very good reservoir quality, while the percentage of water saturation indicates petroleum saturation of not less than 90% (Dresser, 1982; Dewan, 1983).

LFA 4: *Middle estuary.* The association of massive or structureless sandstone (lithofacies 6) of tidal bore (Fan et al., 2014; Dalrymple, 2021); channelized medium bedded cross-stratified (lithofacies 8) of tidal channel sandbars; and thickly interbedded sandstone and shale (lithofacies 7) of tidal channel overbank is interpreted as sediment deposition in the central or middle estuary (Table 1; Fig. 3). Lithofacies 8 represents subtidal channel deposit, while lithofacies 7 and 7 represent tidal current maximum and turbidity maximum in the middle estuary channel (Flemming, 2011; Davis Jr and Dalrymple, 2012). The depositional facies consist of reservoirs (sandstone) and flow barriers (shales). The tidal channel overbank facies has a permeability of 1.1 md, a porosity of 13.2% and water saturation as high as 68.2% and, therefore, serve as intra-reservoir flow barrier. The tidal-bore and tidal channel sandbar deposits of the middle estuary are well-sorted sandstones and formed very excellent-quality petroleum reservoirs with permeability, porosity and water saturation that ranged from 3538.7 to 6720 md, 26.4 to 30.18%, and 6.6 to 25.2%, respectively (Dresser, 1982; Dewan, 1983).

LFA 5: *Outer estuary or estuary mouth.* The association of cross-bedded sandstone (lithofacies 4) characterised by abundant reactivation surfaces and bioturbated heterolithic mudstone (lithofacies 5), interpreted as tidal sandbars and intertidal flats, respectively, indicates deposition in the outer estuary or estuary mouth (Table 1; Fig. 3) (Amos; 1995; Dalrymple and Choi, 2007). The intertidal flat facies has cores with permeability and porosity values of 1630 md and 17.0%, respectively. The good porosity compared to excellent permeability suggests poor correlation that can result in the facies serving as baffles in the D1 sandstone reservoir fluid flow. Whereas, the well-sorted tidal sandbars' sandstone facies of the outer estuary formed a petroleum reservoir of an excellent, good quality with core permeability, porosity and water saturation values of 4834.99 md, 31.02%, and 31.4%, respectively (Dresser, 1982; Dewan, 1983).

LFA 6: *Transgressive tide-dominated shoreface.* The mud-draped, thinly cross-laminated sandstone to muddy sandstone (lithofacies 3) characterised by *Ophiomorpha* burrows is interpreted to be deposited in a transgressive shoreface environment (Table 1; Fig. 3) (Dalrymple et al. 1994). The mud drapes can act as baffles to fluid flow, but generally, the shoreface sandstone facies formed a very good petroleum reservoir with permeability, porosity and water saturation values of 3786.1 md, 30% and 12.3%, respectively.

LFA 7: *Transgressive offshore transition zone.* The bioturbated sideritic mudstone (lithofacies 2) overlying mud-draped fine-grained sandstone is interpreted to be deposited in a transgressive offshore transition zone (Table 1; Fig. 3) (Nichols, 2009). It has an upward-increasing gamma ray log value that ranges from 65 to 95 API (Fig. 2). The depositional facies has permeability, porosity and water saturation values of 949 md, 27% and 40.1%, respectively. The very good permeability and porosity values can be attributed to the effect of moderate to intense bioturbation. Therefore, although there are no visible burrows on the lithofacies, bioturbation that enhanced the storage and flow capabilities of the facies also indeed exposed the sediment to oxidation for siderite precipitation (Tucker, 2003). That is why the lithofacies is named in this study as "bioturbated sideritic mudstone" instead of just "sideritic mudstone" given by Oyanyan and Oshinowo (2026). Furthermore, as the immediate mudstone facies that bounds the D1 sandstone reservoir on top, its water saturation of 40.1% is an indication of almost 60% richness in petroleum and buttressed the

wireline log interpretation of the D1 sandstone reservoir as an oil-up-to reservoir.

LFA 8: *Transgressive offshore.* The dark grey mudstone (Lithofacies 1) overlying bioturbated sideritic mudstone is interpreted to represent deposition in a transgressive offshore estuarine environment (Table 1; Fig. 3) (Dalrymple et al., 1994). It has gamma ray values that range from 95 to 150 API, typical of pure mudstone (Fig. 2) (Dewan, 1983). The depositional facies is a non-reservoir for petroleum with permeability, porosity and water saturation values of 0.2 md, 7.5% and 81.8%, respectively. The lack of permeability shows the facies as a perfect seal for the petroleum-rich D1 sandstone reservoir.

3.2.3 Heterogeneity in cores' permeability and porosity values

The evaluation of permeability and porosity relationships enhanced the understanding of heterogeneity in reservoir quality (Oyanyan and Oti, 2016; Mondal et al., 2017). Only 5.08% of the 61 samples analysed have poor permeability and porosity values and are considered non-reservoirs. Figure 4 shows permeability values that range from 0.1 to 10410 md, a mean value of 3937.1 md and a very broad distribution. The permeability of 95% of the D1 sandstone ranged from good (>50 md) to excellent (>1000 md) (Dresser, 1982).

In porosity distribution, a normal distribution is given by a homogeneous reservoir, while a skewed broad distribution represents a heterogeneous reservoir zone (Hurst and Archer, 1986). The porosity histogram and cumulative frequency distribution show broad normal porosity distribution, indicating a heterogeneous reservoir with values that range from 7.2 to 34.3% (Fig. 5). Generally, the mean porosity of 28.2% in D1 sandstone reservoir indicates very good petroleum storage capability.

Figure 6 shows the permeability distribution and Dykstra-Parson coefficient plot of the D1 sandstone reservoir. The Dykstra-Parson coefficient of variation (*Vdp*) of 0.84 indicates that the reservoir deposit is heterogeneous with an intra-sandbody compartmentalization potential. Though the reservoir is heterogeneous, the permeability distribution shows that only three samples have values less than 50 md, indicating that DI sandstone interpreted as tide-dominated estuarine sandstone reservoir is generally a good to excellent reservoir for petroleum. The heterogeneity in the petroleum-rich reservoir is further substantiated with the normal probability plot of the irreducible water saturation (SWi) that indicates eight rock types with eight distinct straight lines (Fig. 7). It is documented that irreducible or connate water saturation has causative inter-relations with permeability and capillary pressure (Widarsono, 2011). As shown in Fig. 7, only eight samples out of sixty-one samples have irreducible water saturation that is more than 50%, but the values of the irreducible water saturation, an intrinsic property of the reservoir, show that the storage capacities for petroleum vary across the eight rock types.

Figure 8 shows the cross-plot of permeability and porosity values. The plot shows permeability values that are up to about four orders in magnitude and a range of permeability and porosity values that suggest very good to excellent reservoirs (Dresser, 1982). But the regression coefficient (R) value of 0.27 is an indication of poor correlation between porosity and permeability. The poor correlation between the cores' permeability and porosity values substantiates the fact that permeability values are not only dependent on porosity but also dependent on other depositional characteristics such as grain size, pore geometry and tortuosity, which is affected by diagenetic factors such as cementation, compaction, mineral precipitation and solution (Khalid et al., 2020). These characteristics are possibly responsible for the poor correlation coefficient and heterogeneity, necessitating detailed characterisation of the reservoir up to the pore-scale level using Winland and hydraulic unit rock-typing methods.

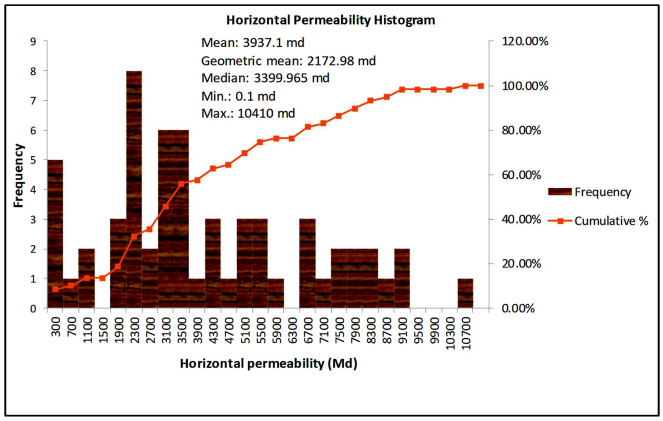


Figure 4: Permeability histogram of all lithofacies

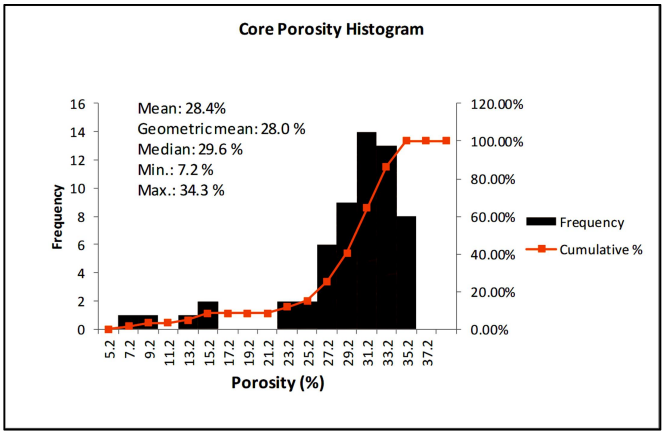


Figure 5: Porosity histogram of all lithofacies.

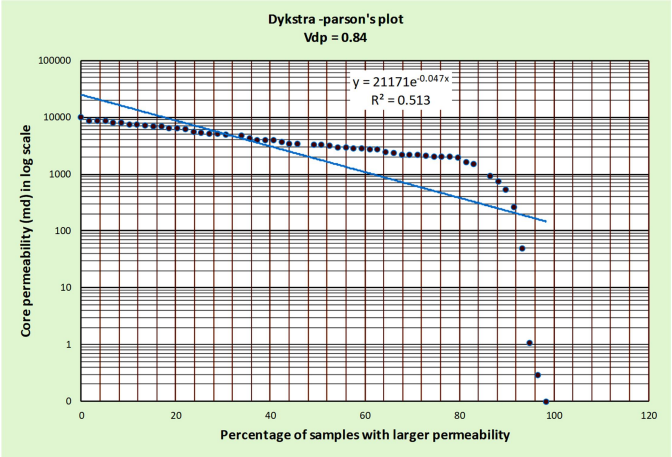


Figure 6: Permeability distribution and Dykstra-Parson coefficient of core permeability variation in D reservoir sandstone. The coefficient of variation (Vdp) of 0.84 indicates that the reservoir is vertically heterogeneous.

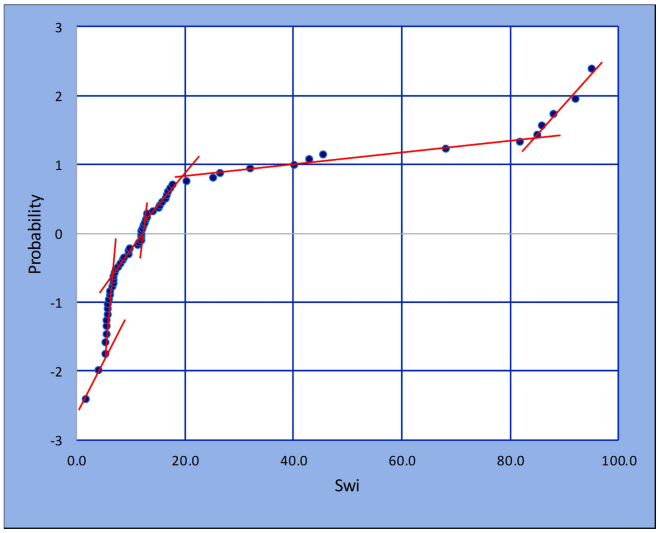


Figure 7: Normal probability plot of irreducible water saturation (S_{Wi}) with the 8 distinct straight lines indicating 8 rock types in D1 sandstone reservoirs, It shows variability in petroleum storage capabilities across the eight rock types.

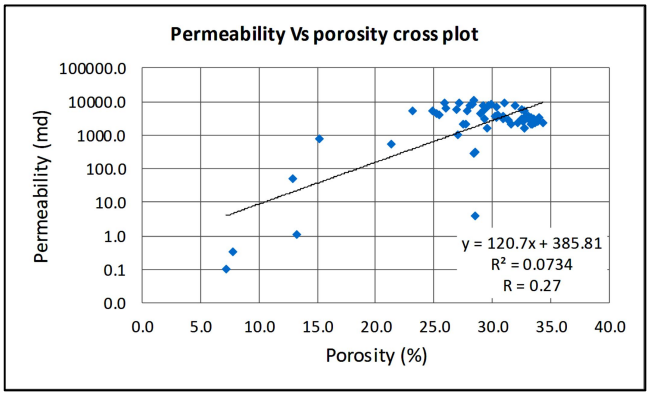


Figure 8: Permeability-Porosity Plot for D1 sandstone reservoir

3.3 Microscopic heterogeneities

Microscopic heterogeneities are expressed in terms of pore and pore throat sizes and create preferential flow paths that result in the flow of displacing fluids while some residual or trapped oil is left behind (Ravalec et al., 2014). Rock-type determination at pore scales through the following methods gave an enhanced reservoir quality description and revealed the microscopic heterogeneities in the D1 sandstone reservoir.

3.3.1 Winland R35 rock types

The application of equation 2 on the D1 sandstone facies cores' porosity and permeability data resulted in the classifications of the reservoir into microporous (0.2 - 0.5 µm), mesoporous (0.5 - 2 µm), macroporous (2.0 - 10 µm), and megaporous (>10 µm) rock types based on the empirical pore-throat (R35) values calculated (Fig. 9). The calculated pore throat sizes vary across the lithofacies, with the lowest value recorded for the dark grey mudstone of offshore and the highest recorded for the massive bedded sandstone of tidal-bore

deposits at middle estuary and followed by the cross-bedded sandstone of tidal sandbars of outer estuary depositional environments (Table 2). The microporous rock types which form intra-reservoir flow barriers are only 3.45%, while the mesoporous, macroporous and megaporous types constitute 1.7%, 5.17% and 89%, respectively. The average pore-throat size is 34.32 µm and suggests a general high-quality reservoir with well-sorted and connected pores. Even though 89% of the reservoir is megaporous and of general high quality, the normal probability plot of irreducible water saturation has already established variability in petroleum storage capabilities across eight rock types (Fig. 7).

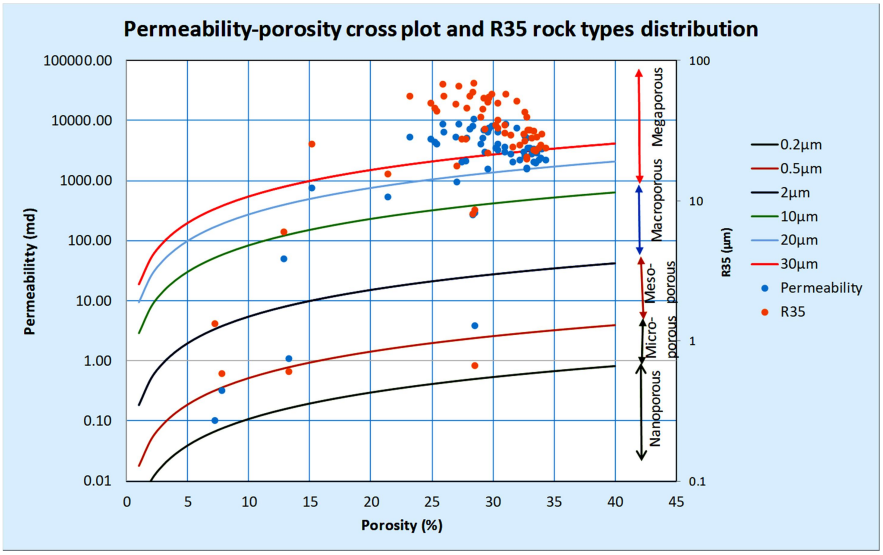


Figure 9: Winland plot for D1 sandstone reservoir showing various pore types

Table 2: Mean pore throats variations with lithofacies and comparison with mean core porosity and permeability

Lithofacies No.	Lithofacies	Mean Porosity (%)	Mean Permeability (md)	Mean R35 (µm)
1.	Dark grey mudstone	7.5	0.2	0.37
2.	Bioturbated Sideritic mudstone	27.0	949	22.27
3.	Mud-draped cross laminated sandstone	30.6	3786.1	35.67
4.	Cross bedded sandstone	31.02	4834.99	40.70
5.	Heterolithic mudstone.	17.0	1630	0.82
6.	Massive bedded sandstone	26.4	6720	56.78
7.	Thickly interbedded sandstone and shale	13.2	1.1	0.51
8.	Channelized medium bedded cross-stratified sandstone.	30.18	3538.7	33.83
9.	Horizontal bedded sandstone	26.85	2222.25	28..23
10.	Heterolithic sandstone.	33.4	1990	22.66
11.	Channelized thinly cross laminated sandstone.	26.2	1807.5	26.41
12.	Heterolithic shale	28.3	3.9	0.42

3.3.2 Hydraulic units' rock types

Reservoir quality index (RQI), zone or index porosity (Φz) and flow zone indicators (FZI) values of the D1 sandstone reservoir were calculated with Equation 3-5. The graphical clustering using the classical RQI-Φz plot of Amaefule *et al*. (1993) was first attempted to group the FZI into Hydraulic Units (HU) as shown in Fig. 10. Five different clusters of data represented with parallel lines, with each line of data set having similar flow zone indicators (FZI), were identified. The five clusters of data are hydraulic units (HUs), where HU with FZ1 values between 0.03 and 0.06 µm are non-reservoirs, while FZI values between 0.24 and 1.4 µm are reservoirs (Fig. 10). But most of the FZI data points are packed between lines of 0.5 and 1.24 µm and are not clustered along any parallel lines. Consequently, normal probability plotting of the FZI value was used to identify clusters in which all data are in distinct lines.

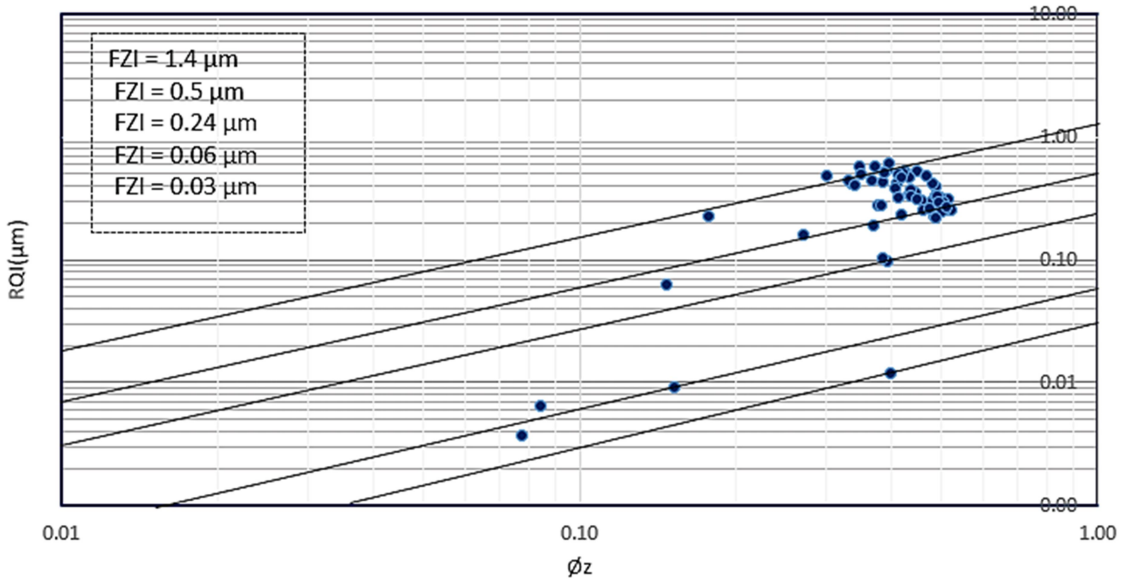


Figure 10: Plot of RQI vs OZ for five Hydraulic Flow Units (HFU) from the averaged Flow Zone Indicators (FZI) through graphical groupings.

As shown in Fig. 11, there are eight distinct lines in the normal probability plot, indicating eight hydraulic unit (HU) rock types. The lower boundary of each distinct straight line was used as the lower boundary of the flow zone indicators of hydraulic (flow) units (HU) (Table 3). The FZI of the lower boundaries and zone porosity (Φz) values calculated using equation 5 and the cores' porosity (ϕe) were substituted into equation 6 to predict or calculate the permeability values corresponding to the lower boundaries of the HUs. The graphical plotting of the predicted permeability values against the cores' porosity (ϕe) values in fraction was merged with the cross-plot of cores' permeability and porosity in fraction values to have the cores' permeability values perfectly segregated into eight hydraulic units, as shown in Fig. 12. Because almost ninety per cent of D1 sandstone reservoirs have been classified as megaporous, the hydraulic units (HU) rock types 1 with FZI greater than 1.52 µm were classified as very excellent hydraulic flow units (HFU); HU rock type 2 with FZI of 1.28 µm as excellent HFU, while HU rock types 3 and 4 with FZI of 1.6 – 1.0 µm as very good HFU and HU rock types 5 and 6 of FZI 0.4 – 0.6 µm as good HFU, and HU rock types 7 and 8 of FZI of 0.24 and 0.03 µm as baffles and non-reservoir rocks/flow barriers, respectively (Table 3). Eighty-nine per cent of D1 sandstone

reservoirs ranged from good to excellent hydraulic flow units. The eight hydraulic flow units are in sync with the eight rock types predicted with the normal probability plot of the irreducible water saturation values.

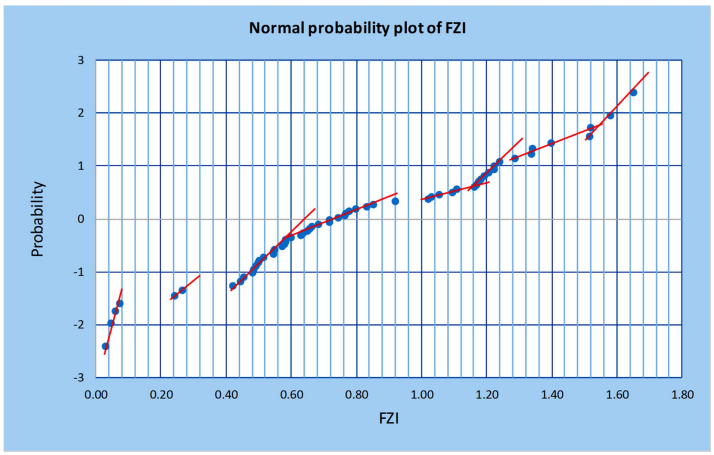


Figure 11: Normal Probability plot of flow zone indicators, with the distinct straight lines indicating different rock types and the eight lower boundaries for the classification of eight hydraulic units rock types.

Table 3: Hydraulic units rock types, flow zone indicators lower boundaries and percentage of rock type.

HU rock types	FZI (μm) lower boundaries	Percentage of rock type (%)	Classification of Hydraulic flow unit (HFU)
1.	1.52	6.4	Vey excellent
2.	1.28	6.4	Excellent
3.	1.16	14.5	Very good
4.	1.0	6.4	
5	0.6	32.3	Good
6	0.4	22.6	
7	0.24	3.2	Non-reservoirs /flow barriers or baffles
8	0.03	8.1	

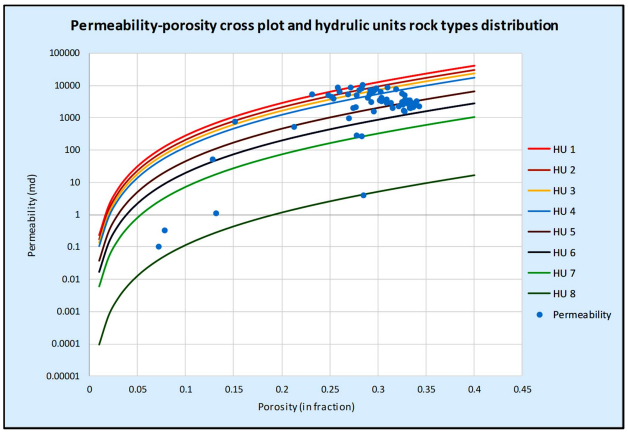


Figure 12: The classification of 62 flow zone indications into 8 hydraulic units.

3.3.3 Correlation of rock types against each other and depth

The cross-plot of r35 and flow zone indicator values (Fig. 13) indicates a very high correlation with a regression coefficient of 0.95 (R^2 = 0.90). This indicates that both the Winland R35 and flow zone indicator methods produce good definitions of flow capacities of reservoir units, and any of the two methods can be used for rock typing (Rushing *et al.*, 2008). Similarly, the plotting of r35, flow zone indicators and core permeability values against depth perfectly shows strong correlation (Fig. 14). It validates the popular concept that the intrinsic reservoir permeability depends on pore structure and pore-throat size distribution (Widarsono, 2011).

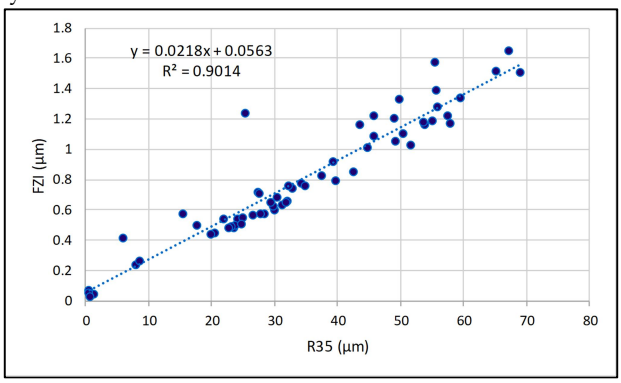


Figure 13: Cross plot of R35 values and flow zone indicators showing very high correlation between flow zone indicator and r35 values.

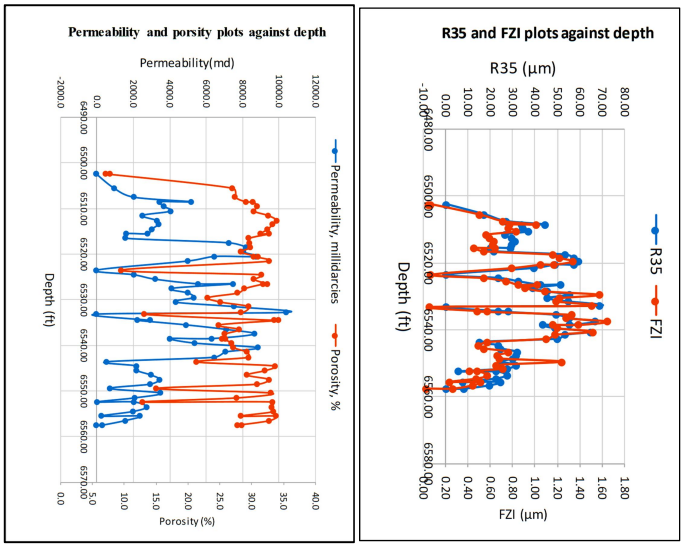


Figure 14: The plot of prosity, permiability, r35 and flow zone indicators show very good correlations among the three parameters.

3.4 Depositional Control on Hydraulic Flow Units Distribution and reservoir quality

The identified hydraulic (flow) units (HFU) rock types are related to geological facies, but they do not coincide with boundaries. In some single depositional facies or sub-environments of deposition, you have several hydraulic unit rock types, and some single lithofacies are characterised by a range of hydraulic unit rock

types (Table 5). The best HFU with FZI greater than 1.52 μm is the massively bedded sandstone facies of tidal-bore deposition at the middle estuary. Similarly, the non-reservoir/flow-barrier hydraulic rock types, HU 7 and 8, are only the deposits of the offshore transition zone to offshore depositional environments. As shown in Table 5, HU rock types 2 – 5 are found in lithofacies 4 (cross-bedded sandstone), suggesting that tidal sandbars deposited in estuary mouths form good to excellent HFUs. Similarly, HU rock types 2-4 are found in lithofacies 8 (channelized medium bedded cross-stratified sandstone), suggesting that tidal channel sandbars deposited in the middle and inner estuary form very good to excellent HFU. Similarly, lithofacies 3 (mud-draped cross-laminated sandstone) is characterised by HU rock types 4 and 5, suggesting that the transgressive shoreface deposit produces good to very-good HFU despite the mud drapes. The variability of HFU across the different lithofacies suggests the energy of the depositional environment as the principal control of the reservoir quality distribution. As shown in Fig. 15, the plot of the hydraulic units (HU) against depth suggests the control of tidal current speed and energy on the distribution of HFUs in the D1 sandstone reservoir. The plot shows five cycles of increase and decrease in the quality of HU rock types that clearly mimic fluctuation in tidal current speed and energy. Each peak of the five cycles corresponds to the deposition of HUs 1-4, classified as very good to excellent HFUs (Table 3). The highest peak among the five cycles corresponds to the deposition of HU1, formed by lithofacies 6 (massive bedded sandstone), interpreted as tidal-bore deposition. A tidal bore has been defined as a moving hydraulic jump, triggered by a rushing flood tide into a funnel-shaped river mouth (fan et al., 2014; Dalrymple et al., 2021). Therefore, a tidal-bore deposit is an indication of a zone of tidal current speed and energy maximum in an estuary. Similarly, most troughs of the cycles correspond to the deposition of HU rock type 8 classified as non-reservoirs/flow barriers and baffles (Table 3). The HU 8 is formed by lithofacies 12 (heterolithic shale) and 1 (dark grey mudstone), interpreted as low-energy deposition in the offshore transition zone and offshore, respectively.

Table 5: Distribution of hydraulic unit rock types in lithofacies

HU rock types	FZI (μm) lower boundaries	Lithofacies Numbers	Lithofacies types
1.	1.52	6	Massive bedded sandstone.
2.	1.28	4, 6, 8	Cross bedded sandstone, Massive bedded sandstone and Medium bedded cross-stratified sandstone.
3.	1.16	4, 6, 8, 9	Cross bedded sandstone, Massive bedded sandstone, Medium bedded cross-stratified sandstone and Horizontal bedded sandstone
4.	1.0	3, 4, 6, 8	Mud-draped cross laminated sandstone, Cross bedded sandstone, Massive bedded sandstone and Medium bedded cross-stratified sandstone.
5	0.6	3, 4, 9	Mud-draped cross laminated sandstone, Cross bedded sandstone and Horizontal bedded sandstone
6	0.4	2, 5, 8, 9 10, 11	Bioturbated Sideritic mudstone, Heterolithic mudstone, Medium bedded cross-stratified sandstone and Horizontal bedded sandstone, Heterolithic sandstone and Thinly cross laminated sandstone.
7	0.24	12	Heterolithic shale
8	0.03	1, 12	Dark grey mudstone and Heterolithic shale

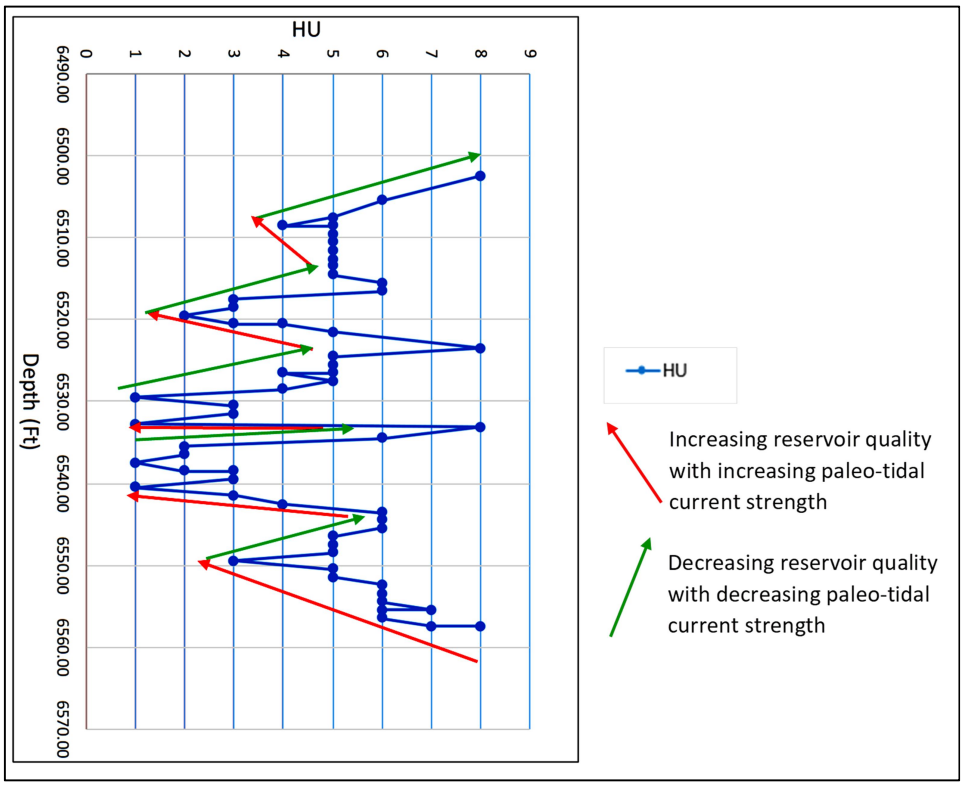


Figure 15: The plot of hydraulic units rock types against depth suggest the control of fluctuating tidal energy on reservoir quality. It suggests the influence of five major cycles of tidal energy fluctuations in the deposition of D1 sandstone reservoir.

3.5 Intra-sand body Compartmentalization and Well Perforation Guide for optimum petroleum production

The optimisation of petroleum from a petroleum-rich reservoir requires perforating the appropriate depth interval during well development and applying other engineering procedures that can result in high sweep efficiency in both areal and vertical dimensions. Therefore, petroleum production optimisation is steadily decreasing the non-swept zones in a reservoir to a minimum or zero and increasing the swept zone to the maximum, or a hundred per cent of the reservoir, with no bypassed oil pool. Therefore, the plotting of hydraulic units (HU) rock types against depth resulted in the identification of three intra-reservoir compartments that can serve as a guide in the well perforation, as shown in Fig. 16. Perforating the depth interval with the best HU in each compartment will result in optimum petroleum recovery as petroleum migrates from low elevation zone to the higher elevation zone and from the high-pressure zone to the low-pressure zone in the wellbore.

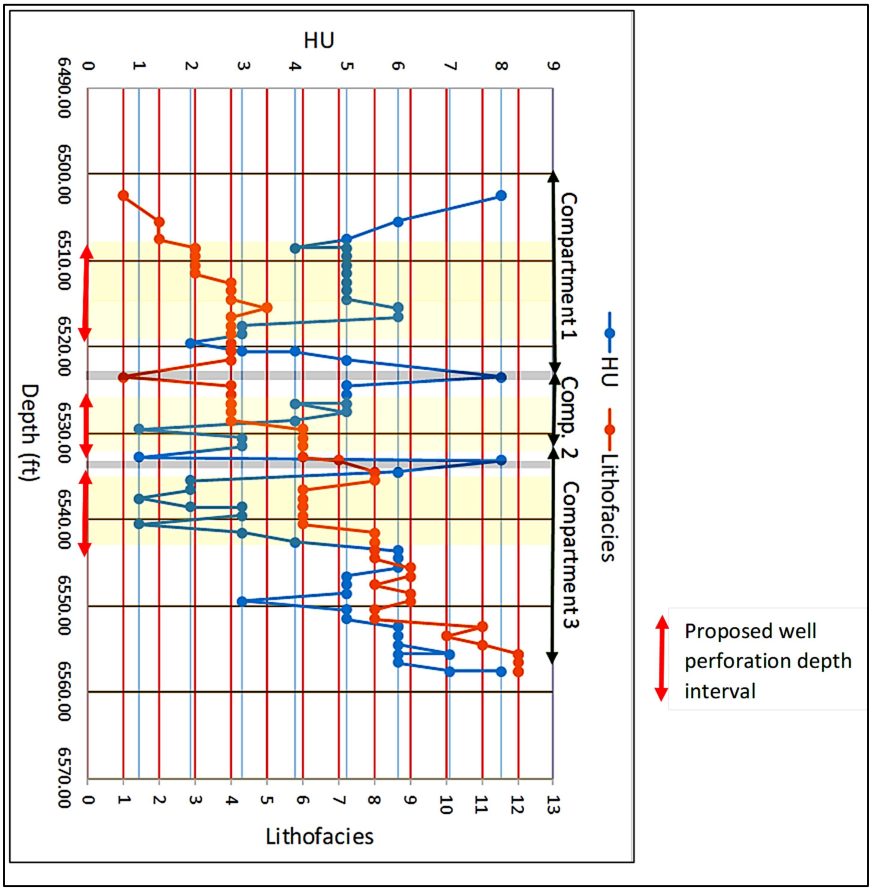


Figure 16: Intra sand-body compartmentalization scheme of D1 sandstone reservoir showing vertical distribution of lithofacies, three compartments and vertical layering that can be used as a guide for well perforation for optimum petroleum production.

3.4 The predicted hydraulic flow units in the non-cored D1b reservoir in Well 01

As indicated in section 3.1.2, the D1b sandstone reservoir also consists of petroleum in Well 01, with a defined oil-water contact at 7304 ft (Fig. 2). To optimally drain the reservoir, the permeability (K), R35 and HU distributions in the reservoir were predicted using multiple linear regression (MLR) models trained with the data from the cored D1 sandstone reservoir in well 13 (Table 6). Among the bulk density and gamma ray logs, the latter was found to be the most statistically significant predictor. As shown in Table 6, MRL statistics show that the three models are statistically significant, with significant F far less than 0.05 (Draper and Smith, 1998). But FZI and R35 predictive models have the highest multiple regression coefficient (R) of 0.75 and are considered very good predictive models, and their predictive values were found to be reliable for hydraulic flow unit layering in the D1b sandstone reservoir.

The predicted R35 and FZI values show that the pore-throat sizes and HU in the D1b sandstone reservoir of well 01, respectively, are mainly megaporous, and hydraulic flow units are good to very good (Fig. 17). Perforating the depth interval with the best HUs and far above the oil-water contact, as indicated in Figure 17, will result in optimum recovery of oil from the 14 ft (4.27 m) net-thick reservoir.

Table 6: Multiple linear regression (MLR) algorithms and statistics

Dependent variable	Multiple R	R square	F	Sig. F	MLR Algorithms
K (md)	0.67	0.45	24.37	<0.005	$K=4700.251-65.6177*\gamma+1178.017*\rho_b$
R35	0.75	0.56	37.59	<0.005	$R35 = 38.760-0.489*\gamma +9.74534*\rho_b$
FZI	0.75	0.56	37.55	<0.005	$FZI=0.59008-0.01133*\gamma + 0.375812*\rho_b$

γ = Gamma ray log value. ρb = bulk density log value. K = Permeability

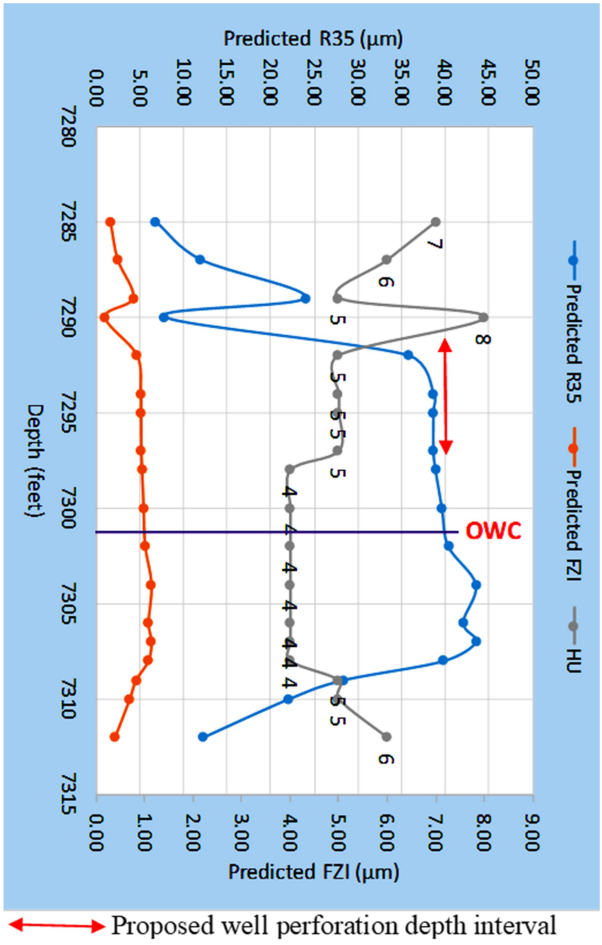


Figure 17: Shows the plot of the predicted values of R35, FZI and HU against depth; oil water contact (OWC) and the proposed well perforation depth interval in D1b sandstone reservoir of Well 01.

4. DISCUSSION

This study has shown the infill stratigraphy of a tide-dominated estuary, a summary of processes of the infill deposition, factors that control the deposition and the heterogeneities in rock types and petrophysical properties of the infilled deposits. The infilled stratigraphy evinces layer-cake architecture due to the influence of sea-level fluctuations on the sediment deposition, typical of the Niger Delta basin coastal deposits (Weber and van Geuns, 1990; Larue and Legarre, 2004; Reijers, 2011). An abrupt increase in sea level resulted in the deposition of field-wide flooding surface shales, the main element of macroscopic heterogeneities responsible for the vertical subdivision of the D sandstone reservoir into inter-parasequence compartments.

In line with Oyanyan and Oshinowo (2026), the impoverished ichnofossil suite in all the

identified depositional facies, the abundant reactivation surfaces in tidal sandbars of the outer estuary, the tidal-bore deposits in the middle estuary and the tidal ravinement surface in the inner estuary in the study-cored D1 sandstone reservoir suggest deposition in a tide-dominated estuary. The twelve lithofacies that described the core samples are an indication of megascopic and mesoscopic heterogeneities that can be attributed to the combination of variations in depositional process, relative sea levels and tidal current speed/energy (Ravalec et al., 2014). Generally, the sandstone facies' grains are mostly well sorted and hence characterised by good to excellent storage and flow capacities with mean permeability and porosity values of 3937.1 md and 28.1%, respectively. The sorting of sediment grains that determines the quality of a reservoir depends on the source/distance of travel and the winnowing energy of the depositional environment (Nichols, 2009). The well-sorted D1 sandstone's grains, therefore, suggest reworked sediment supply. Typical estuary environments receive sediments from both marine and fluvial sources (Darymple et al., 1992; Tessier, B. 2012). It therefore also suggests that the estuary received sediment reworked from slightly older distributary-mouth-bar deposits, and according to Dalrymple and Choi (2006), such an estuary is classified as a delta-plain estuary.

Microscopic heterogeneities in the D1 sandstone reservoir are indicated by eight hydraulic unit (HU) rock types with different amounts of irreducible water saturation. The tidal-bore deposit of the middle estuary gave the best HU, followed by tidal sandbars of the outer estuary, to show the sedimentary facies control on reservoir quality, fluid behaviour, and porosity and permeability heterogeneities (Buatois et al., 1999). In the depositional processes of the reservoir, tidal current speed/energy fluctuation mainly controlled the distribution of the hydraulic flow units (HFU). The highest-quality reservoir, the tidal-bore deposit, is associated with the rapid deposition of sediment resuspended by the highest tidal energy, while the non-reservoir rock types are deposits associated with either slack tidal flow or general low-energy depositional conditions. The vertical distribution of the hydraulic units in the D1 sandstone reservoir is in line with the tidal range and tidal-current speed variations along the length of an estuary, which also mimic longitudinal changes in tidal energy. Tidal range and tidal-current speeds increased from the estuary mouth to the middle estuary because of the progressive decrease in cross-sectional area of the estuary channel, but at a certain point they decreased to zero at the tidal limit in the inner estuary due to friction on the bottom and sides (Dalrymple and Choi, 2006).

The highest-quality hydraulic rock types have the largest pore-throat size network (Amaefule et al., 1993; Rushing et al., 2008). Therefore, perforating the depth interval of the best HU in any reservoir compartment is a good option for an optimum petroleum reservoir. Since oil well coring attracts a huge cost and consequently not all oil wells are cored, predicting the HFU in the non-cored wells using MRL algorithms or any other machine learning algorithm is a necessary option for optimum petroleum recovery.

5. CONCLUSIONS

The following conclusions can be drawn from this study:

1. The study cored D1 sandstone reservoir was deposited in a tide-dominated estuary, as indicated by the impoverished ichnofossil suite in all the depositional facies, the abundant reactivation surfaces in tidal sandbars of the outer estuary, the tidal-bore deposits in the middle estuary and the tidal ravinement surface in the inner estuary.

2. The quality of the tide-dominated estuary reservoir was controlled by tidal current speed and energy fluctuations, as indicated by the plotting of hydraulic units against depth.

3. The entire D sandstone reservoir is characterised by megascopic to microscopic heterogeneities that resulted in inter-parasequence and inter-sand-body reservoir compartmentalizations as well as intra-sand-body compartmentalization.

4. Despite the high level of heterogeneities, the tide-dominated estuary formed a good- to excellent-quality reservoir due to moderate- to very-good sorting of grains.

5. The vertical layering of the hydraulic flow and the perforation of the depth interval with the best hydraulic unit rock types during well development present an opportunity to optimally drain the petroleum-rich heterogeneous reservoir with high sweep efficiency.

6. Finally, with machine learning algorithms such as multiple linear regression, the flow zone indicators and hydraulic flow unit of the D1 reservoir in a distant non-cored well can be predicted to optimally drain the reservoir that is not in pressure communication with the cored well due to heterogeneities.

DECLARATIONS

Ethics approval and consent to participate

Not applicable

Consent for publication

Not applicable

Competing interests

The author declared no competing interest concerning the research, authorship, and/or publication of this article.

Funding

There was no funding for this research.

Availability of data and material

The data analysed and interpreted in this study are dataset generated by an Oil and Gas company and therefore not publicly available. The dataset is only available from the corresponding author upon very reasonable request.

Authors contribution

Raphael Oaikhena Oyanyan: Develop the research concept, designed the aim and methods of study, prepared and interpreted the data, prepared figures, wrote the manuscript and edited the manuscript.

References

Abbaszadeh, M., Fujii, H. & Fujimoto, F. (1995). Permeability Prediction by Hydraulic Flow Units-Theory and Applications. SPE March Petrovietnam Conference, Hochiminh, Vietnam, 1-3, Paper SPE 30158.

Ainsworth, R.B. (2010). Prediction of stratigraphic compartmentalization in marginal marine reservoirs. Geol. Society, London, Special Public., 347, 199-218. DOI: 10.1144/SP347.12.

Amaefule, J.O., Altunbay, M., Tiab, J., Kersey, D. G. & Keelan, D. K. (1993). Enhanced reservoir description: Using core and log data to identify hydraulic (Flow) units and predict permeability in uncored intervals/wells. Proceedings of the Oct. 3-6, 68th Annual Technical Conference and Exhibition, Houston, Texas, pp. 16-16.

Amos, C. L. (1995). Siliciclastic tidal flat. In: Perillo, G. M. E. (Eds.), Geomorphology and sedimentology of estuaries. Developments in Sedimentology, 53, 273-306.

Bello, A. M., Usman, M. B., Amao, A. O., Al-Ramadan, K., Al-Hashem, M., Kachalla, A., Abubakar, U., Salisu, A.A., Mukkafa, S., Kwami, I. A., Aro, O. E., Butt, M. N., Maigari, A. S., Yusuf, A., Chiroma, L. U. & Akinsanpe, O. T. (2024). Diagenesis and reservoir quality evolution of estuarine sandstones: Insights from the Cenomanian-Turonian Yolde Formation, northern Benue Trough, NE Nigeria, Marine and Petroleum Geology, 169, 107073. ISSN 0264-8172. https://doi.org/10.1016/j.marpetgeo.2024.107073.

Boada, E., Barbato, R., Porras, J. C. & Quaglia, A. (2001). Rock typing: Key approach for maximizing use of old well log data in mature fields, Santa Rosa field, case study. Proceedings of the Mar. 25-29, Latin American and Caribbean petroleum Engineering Conference, Buenos Aires, Argentina, pp: 7-7. DOI: 10.2118/69459-MS.

Buatois, L. A., Mángano, M. G. & Carr, T. R. (1999). Sedimentology and Ichnology of Paleozoic Estuarine and Shoreface Reservoirs, Morrow Sandstone, Lower

Pennsylvanian of Southwest Kansas, USA, 241, 1- 35.

Cant, D. J. (1992). Subsurface Facies Analysis. In: Walker, R. G. and N. P. James (Eds.), Facies Models: Response to Sea Level Change. Geological Association of Canada, St., John's, Nfld, pp. 1- 409, ISBN: 0919216498.

Catuneanu, O. (2006). Principles of Sequence Stratigraphy. Elsevier, Amsterdam, pp. 1-386.

Dalrymple, R. W. and Choi, K. (2007) Morphologic and facies trends through the fluvial–marine transition in tide-dominated depositional systems: A schematic framework for environmental and sequence-stratigraphic interpretation. Earth-Science Reviews, 81,135–174. doi:10.1016/j.earscirev.2006.10.002.

Dalrymple, R.W. (2021). Sedimentation on high-energy sand flats in the Bay of Fundy: The record of tidal-bore activity and deposition from high concentration suspensions of sand. Sedimentology, 68, 2195–2226. John Wiley & Sons Ltd Publication on behalf of International Association of Sedimentologists. doi: 10.1111/sed.12851.

Dalrymple, R.W., Boyd, R. & Zaitlin, B.A., (Eds.), (1994). Incised Valley Systems: Origin and Sedimentary Sequences. SEPM, Special Publication 51, pp. 1-391.

Dalrymple, R.W., Zaitlin, B.A. & Boyd, R. (1992). Estuarine facies models: conceptual basis and stratigraphic implications. J. Sed. Petrol. 62, 1130–1146.

Davis Jr, R.A. and Dalrymple, R. W. (2012). Principles of Tidal Sedimentology. 1st Edn., Springer Netherlands, ISBN-10: 978-94-007-0123-6, pp. 1-621.

Dewan, J.T. (1983) Essentials of modern open hole log interpretation. Pennwell publishing company Oklahoman, pp. 1-361.

Doust, H. and Omatsola, E. (1989). Niger Delta, *in* Divergent margin basins, J. D. Edwards and P. A. Santogrossi, eds., AAPG Memoir, 48,201-238.

Draper, N.R. and Smith, H. (1998). Applied Regression Analysis. 3rd Edn., Wiley and Sons, New York, ISBN-10: 0471170828, pp. 1- 706.

Dresser, A. (1982). Well Logging and Interpretation Techniques: The Course for Home Study. 2nd Edn., Dresser Atlas, pp. 1- 492.

Dykstra, H. and Parsons, R. L. (1950). The Prediction of Oil Recovery by Waterflood. In: Secondary Recovery of Oil in the United States, API and DP, American Petroleum Institute, New York, pp: 160-174.

Ejedawe, J. E. (1981). Patterns of incidence of oil reserves in Niger Delta Basin. American Association of Petroleum Geologists bulletin, 65, 1574-1585.

Fan, D., Tu, J.& Shang, S., Cai, G. (2014). Characteristics of tidal-bore deposits and facies associations in the Qiantang Estuary, China. Marine Geology, 348, 1–14. Elsevier B.V Publications. http://dx.doi.org/10.1016/j.margeo.2013.11.012.

Flemming, B.W. (2011). Geology, morphology and sedimentology of estuaries and coasts. In: Flemming, B.W., Hansom, J.D. (Eds), Treatise on Estuaries and Coasts, Volume 3, Estuarine and Coastal Geology and Morphology. Elsevier, Amsterdam, pp. 7–38.

Galloway, W. E. and Hobday, D. K. (1996). Terrigenous clastic depositional systems: Applications to fossil fuel and ground water resources: Springer-Verlag, Berlin, pp.1-491.

Gunter, G., Finneran, J., Hartmann, D. & Miller, J. (1997). Early Determination of Reservoir Flow Units Using an Integrated Petrophysical Method. SPE38679, pp. 1-8.

Hurst, A. and Archer, J. S. (1986). Sandstone reservoir description; an overview of the role of geology and mineralogy. Clay Minerals, 21, 791-809.

Jensen, J. J., Lake, L. W., Corbett, P. W. M. & Goggin, D. J. (2000). Statistics for Petroleum Engineers and Geoscientists. In: Handbook of Petroleum Exploration and Production, Amsterdam, B.V. (Ed.), Elsevier Science, pp. 338-338.

Jiwei, C., Kexin, Z., Chaoqian, Z., Yunbo, L., Taoran, F., Jian, L., Xianglin, X. & Zhongzhen, M. (2025). A case study of reservoir characterization and

modeling for tidal-dominated estuary reservoir in Ecuador. Scientific Reports, Springer Nature Publ., 15, 19522 https://doi.org/10.1038/s41598-025-03591-7

Khalid, M., Desouky, S. E., Rashed, M., Shazly, T. & Sediek, K. (2020). Application of hydraulic flow units' approach for improving reservoir characterization and predicting permeability. Journal of Petroleum Exploration and Production Technology, 10, 467–479. https://doi.org/10.1007/s13202-019-00758-7

Knox, G. J. and Omatsola, M. E. (1987). Development of the Cenozoic Niger Delta in terms of the escalator regression model. [In:] *Proceedings of the KNGMG Symposium 'Coastal Lowlands-Geology and Geotechnology'*. Kluwer Academic Publishers, pp.181–202.

Kolodzie, S. J. (1980). Analysis of pore throat size and use of the Waxman-Smits equation to determine OOIP in spindle field, Colorado. Proceedings of the 55th, Sept. 21-24, Annual Technical Conference and Exhibition, Dallas, Texas, pp. 10-10. DOI: 10.2118/9382-MS.

Larue, D. K. and Legarre, H. (2004). Flow units, connectivity, and reservoir characterization in a wave-dominated deltaic reservoir: Meren reservoir, Nigeria AAPG Bulletin, 88(3), 303–324.

Lasseter, T.J., Waggoner, J. R. & Lake, L. W. (1986). Reservoir Heterogeneities and Their Influence on Ultimate Recovery. In: Reservoir Characterization, Lake, Jr., L.W. and H.B. Carroll, Academic Press, Orlando, ISBN-10: 0124340652, pp. 545-559.

Mack, G. H., Leeder, M., Perez-Arlucea, M., Brendon D.J. & Bailey, B. D. J. (2003). Sedimentology, Paleontology, and Sequence Stratigraphy of Early Permian Estuarine Deposits, South-Central New Mexico, USA. PALAIOS, SEPM (Society for Sedimentary Geology), 18, 403-420.

Mondal, S., Singh, D. & Das, S. (2017). Enhanced Reservoir Description Using Hydraulic Flow Unit Concept for A Clastic Reservoir: A Case Study of Linch Pay, Linch Field, Cambay Basin, India. SPG india, JAIPUR, pp. 1-7.

Nichols, G. (2009). Sedimentology and Stratigraphy. Wiley and Blackwell Publ. (second edition), pp. 1-432.

Nio, S.-D. and Yang, C. S. (1991). Diagnostic attributes of clastic tidal deposits: a review. In: Smith, D.G., Reinson, G.E., Zaitlin, B.A., Rahmani, R.A. (eds) Clastic Tidal Sedimentology. Canadian Society of Petroleum Geologists, Memoirs, 16, 3–28.

Orlov, M.L. (1996). Multiple linear regression analysis using Microsoft excel. Department of Chemistry, Oregon State University, pp. 1-19.

Owoyemi, A.O. and Willis, B.J. (2026). Depositional patterns across syndepositional normal faults, Niger delta, Nigeria. Journal of Sedimentary Research, 76, 346–363.

Oyanyan, R. O., Ideozu, R. U. & Jackson, C. A. (2023). Sand Thickness Distribution in Crestal (Growth) Faulted Systems Tracts Sediments in an Eastern Coastal Swamp Depobelt Oil Field, Niger Delta Basin, Nigeria. NAPE Bulletin, 32 (2), 10-22.

Oyanyan, R. O. and Oshinowo. O. 0. (2026). Sedimentology and ichnology of estuarine reservoir sandstone deposits in a transgressive systems tract, coastal swamp depobelt, Niger Delta Basin, Nigeria. Discover Geoscience, Springer nature publ, 4, 268. https://doi.org/10.1007/s44288-026-00643-x

Oyanyan, R. O. and Oti, M. N. (2016). Heterogeneities and Intra Sand-Body Compartmentalization in Late Oligocene Delta-Front Deposit, Niger Delta, Nigeria. American Journal of Geosciences (Current Research in Geosciences), Science publ, 6(1), 47 - 64. DOI: 10.3844/ajgsp.2016.47.64. http://thescipub.com/PDF/ajgsp.2016.47.64.pdf

Ravalec, M. L., Doligez, B. & Lerat, O. (2014). Integrated reservoir characterization and modeling. IFP Energies Nouvelles (IFPEN) publ. EAN: 9782901638155. ISBN: 2-901638-15-5. DOI: 10.2516/ifpen/2014001

Reijers, T. J. A. (2011). Stratigraphy and sedimentology of the Niger Delta. Geologos, 17 (3), 133–162.

Rushing, J.A., Newsham, K. E. & Blasingame, T. A. (2008). Rock typing: Keys to understanding productivity in tight gas sands. Proceedings of the Feb. 10-12, Unconventional Reservoirs Conference, Keystone, Colorado, USA, pp. 1-31.

Short, K.C. and Stauble, A.J. (1967). Outline of geology of Niger Delta, AAPG Bull., 51, 761–779.

Smith, W. H. F. and Sandwell, D. T. (1997). Global seafloor topography from satellite altimetry and ship depth soundings: Science, 277, 1957– 1962.

Tessier, B. (2012). Stratigraphy of Tide-Dominated Estuaries In R.A. Davis, Jr. and R.W. Dalrymple (eds.), *Principles of Tidal Sedimentology*, Springer Science+Business Media B.V publications, pp. 1-109. DOI 10.1007/978-94-007-0123-6_6

Tucker, M.E. (2003). Sedimentary Rocks in the Field, Third Edition. John Wiley & Sons Ltd Publ., pp. 1-249.

Weber, K. J. and van Geuns, L. C., (1990). Framework for constructing clastic reservoir simulation models. Journal of Petroleum Technology 42(10),1248–1297.

Weber, K.J. and Daukoru, E. (1975). Petroleum geology of the Niger Delta, *Proc. Ninth World Petrol. Congr.*, 2, 209–221.

Weber, K.J., (1986). How Heterogeneity Affects Oil Recovery. In: Reservoir Characterization. Lake, L.W. and H.B. Carroll Jr. (Eds.), Academic Press, London, ISBN-10: 0124340652, pp. 487-544.

Wendt, W.A., Sakurai, S. & Nelson, P. H. (1986). Permeability Prediction from Well Logs using Multiple Regression. In: Reservoir Characterization. Lake, L.W. and H.B. Carroll Jr. (Eds.), Academic Press, London, ISBN-10: 0124340652, pp. 487-54.

Whiteman, A. (1982). Nigeria- Its petroleum geology, resources and potential: London. Graham and Trotman, pp. 1-394.

Widarsono, B. (2011). Irreducible Water Saturation and Its Governing Factors: Characteristics of Some Sandstones In Western Indonesia. LEMIGAS Scientific Contributions, (34)1, 19-34.

Zhang, W., Huang, J., Feng, W., Wang, L., Shang, H. & Yin, Y. (2022). Reservoir Architecture in Tide-Dominated Estuary: A Case Study of McMurray Formation Oil Sand Reservoir in the Athabasca Block, Canada. Front. Earth Sci. 10:894059. doi: 10.3389/feart.2022.894059